Journal of Power Sources 205 (2012) 1–9

Contents lists available at SciVerse ScienceDirect

Journal of Power Sources

journal homepage: www.elsevier.com/locate/jpowsour

Review

Electrochemical impedance spectroscopy study of Ce(IV) with aminopolycarboxylate ligands for redox flow batteries applications

Portia Modiba[a,b,*], Mangaka Matoetoe[c], Andrew M. Crouch[a,d]

[a] University of Stellenbosch, Department of Chemistry, Private Bag 1, Matieland, Stellenbosch 7602, South Africa
[b] University of Glasgow, Department of Chemistry, Joseph Black Building, Glasgow G12 8QQ, UK
[c] Cape peninsula University of Technology, Department of Chemistry, P.O. Box 652, Zonnebloem 8001, South Africa
[d] University of the Witwatersrand, Faculty of Science, Private Bag 3, Johannesburg 2050, South Africa

ARTICLE INFO

Article history:
Received 5 August 2011
Received in revised form
16 November 2011
Accepted 1 January 2012
Available online 5 February 2012

Keywords:
Electrochemical impedance spectroscopy
Cyclic voltammetry
Redox flow battery
Cerium complexes
Aminopolycarboxylate ligands
Charge/discharge

ABSTRACT

The electrochemical behaviour of cerium with ethylenediamine tetraacetic acid (Ce(IV)–EDTA), ethylenediamine disuccinate (Ce(IV)–EDDS), nitrilotriacetic acid (Ce(IV)–NTA) and diethylenetriamine pentaacetic acid (Ce(IV)–DTPA on a platinum electrode were investigated by cyclic voltammetry (CV) and electrochemical impedance spectroscopy (EIS) for redox flow batteries (RFB) application. The EIS results confirm the results from CV and were in good agreement with obtained data. Ce(IV)–DTPA results show the least resistance and faster electron transfer compared to Ce(IV)–EDTA, Ce(IV)–EDDS, Ce(IV)–NTA. The diffusion coefficient of 1.1×10^{-6} cm^2 s^{-1}, rate constant of 1.6×10^{-4} cm s^{-1}, electrolyte resistance of 1.2 Ω were obtained. A single cell charge/discharge performance of Ce(IV)–DTPA shows as promise for possible application in RFB systems, because of the higher energy and voltage achieved. Therefore, Ce(IV)–DTPA will be a suitable RFB electrolyte compared to Ce(IV), Ce(IV)–EDTA, Ce(IV)–EDDS and Ce(IV)–NTA due to most favoured reversibility and electrochemical properties.

Contents

* Corresponding author at: University of Glasgow, Department of Chemistry, Joseph Black Building, Glasgow G12 8QQ, UK. Tel.: +44 141 330 8233; fax: +44 141 330 4888.
E-mail address: portiam@chem.gla.ac.uk (P. Modiba).

0378-7753/$ – see front matter © 2012 Elsevier B.V. All rights reserved.
doi:10.1016/j.jpowsour.2012.01.004

1. Introduction

The complexes of metals with aminopolycarboxylic acid have received considerable attention in previous years [1–22]. This interest stems mainly from the wide application of these complexes in batteries, superconductors, electrochemical devices, waste-water treatment, industrial, agricultural and analytical applications.

Kinetic and mechanistic studies of electrolytes for redox flow batteries are essential for the identification of suitable electrolytes which display higher potential, upper current and electrochemical reversibility. Currently there are some challenges with the use of redox flow batteries (RBF), namely, mixing of electrolytes, and chemical degradation due to corrosion. An all-vanadium RFB system [23–33] was used to solve some of these challenges due to its various advantages such as the absence of decrease in capacity caused by the cross mixing of the positive electrolyte and negative electrolyte. The introduction of all-vanadium implies that there will be no energy efficiency loss during the process and no cross-contamination of the two half cells electrolyte. Even though these qualities exist for all-vanadium redox flow systems, the open-circuit voltage for each single cell after full charging is about 1.4 V, which is relatively low.

A cerium couple is the most uncomplicated and simple electrolyte for RFB; providing a relatively inexpensive and reliable power source compared to vanadium. In addition it does not cause the cross contamination of the electrolyte in the cell system like vanadium. The oxidation of different organic compounds using carboxylic acids with Ce(IV) has been studied extensively and is currently receiving significant interests [1,3–6]. Abbaspour and Mehrgardi [1] investigated the electrochemical behaviour of Ce(III) ions in the presence of EDTA, and determined kinetic parameters such as transfer coefficient and rate constants for electrocatalytic oxidation of nitrite ion. Lui et al. [34] showed that vanadium can be replaced by cerium in RFB applications. Fang et al. [35] showed that the Ce(IV)/Ce(III) couple has a standard reduction potential of 1.74 V, which is higher than that of all-vanadium RFB. Paulenova and Creager [36] evaluated the cerium couple in a RFB because of its larger positive redox potential, and the cell voltage was predicted to be approximately 1.9 V. Glentworth et al. [2] investigated the kinetics of isotopic exchange reactions between lanthanide ions and lanthanide polyaminopolycarboxylic acid complex ions in aqueous solutions for the chemical effect of nuclear transformations of Ce–EDTA and Ce–DTPA couples.

The Ce^{4+}/Ce^{3+} redox couple is attractive for RFB technology because of its large positive redox potential, which can be developed into a battery with a higher cell voltage and a greater energy storage capacity. Pletcher and Valder [37] reported the electrochemical behaviour of the Ce^{4+}/Ce^{3+} redox couple in aqueous nitrite media, and the electrochemistry of the Ce^{4+}/Ce^{3+} couple in sulphuric acids solution has been widely investigated [3–7,37–39]. To improve those disadvantages and the ratio of power to weight, alternative ligands can be used to complex cerium for example using EDTA, EDDS or DTPA to reach an improved power level. Previous work by Modiba and Crouch [3] used cyclic voltammetry and rotating disk electrodes to evaluate the electrochemical kinetics of Ce(IV)–DTPA and Ce(IV)–EDTA complexes. Ce(IV)–DTPA complex was found to satisfy an important requirement for RFB electrolyte.

This work demonstrates the superior performance of Ce(IV) with the addition of DTPA to form a Ce(IV)–DTPA complex in comparison with other ligands such as ethylenediamminetetraacetic acid (EDTA), ethylenediamminedisuccinic acid (EDDS) and nitrilotriacetic acid (NTA), A search has revealed that there is no electrochemical study of Ce(IV) within the presence of DTPA, EDTA, EDDS, NTA using electrochemical impedance spectroscopy (EIS) for redox flow batteries application. In this paper, we report the study of the Ce(IV) redox system using EDTA or DTPA as a ligand for complexes to be used in redox flow batteries.

2. Experimental

2.1. Materials and reagents

All reagents were of analytical reagent grade unless stated otherwise. ethylenediaminetetraacetic acid (EDTA), ethylenediamine disuccinate (EDDS), nitrilotriacetic acid (NTA) and diethylenetriamine pentaacetic acid DTPA were obtained from (Fluka-Riedel-de Haen) sulphuric acid, potassium ferricyanide ($K_3Fe(CN)_6$), potassium nitrate (KNO_3) sodium hydroxide, cerium (IV) sulphate [$Ce(SO_4)_2$] were purchased from Sigma–Aldrich (Steinheim, Germany).

2.2. Preparation of Ce(IV) with DTPA, NTA, EDDS and EDTA

Cerium (IV) sulphate [Ce(SO4)$_2$] and Ce(IV)–EDTA solutions were prepared as described in the literature [6]. Preparation of the Ce(IV)–DTPA solutions, DTPA was added in the solution instead of EDTA as per literature procedure [6,40] and dissolved in 1 M H_2SO_4 solutions. The solution was filtered, and then poured in a small designed cyclic voltammetry glass cell. Deionized water was prepared by passing distilled water through a Millipore (Bedford, MA, USA) Milli Q water purification system.

2.3. Instrumentation

Cyclic Voltammetry (CV) measurements were performed using a BAS 100B voltammetric System from Bio-analytical Systems Inc., West Lafayette, Indiana, USA. Electrochemical impedance spectroscopy (EIS) measurements were recorded with VoltaLab PGZ 402 (Radiometer Analytical, France) instruments.

2.3.1. Electrochemical measurements

The electrochemical behaviour of Ce(IV) ion in the presence of EDTA, NTA, EDDS and DTPA compound was investigated with cyclic voltammetry and electrochemical impedance spectroscopy. A three-electrode system was used to perform all electrochemical experiments, using platinum electrode with a diameter of 3 mm as a working electrode, Ag/AgCl (3 M NaCl type) as a reference electrode and a platinum wire as a counter electrode.

Impedance measurements were performed in the frequency range from 100 kHz to 100 MHz at potential step from 800 to 1300 mV with applied amplitude of 10 mV. All experiments were performed at room temperature and EIS results were recorded using platinum as working electrode. In all experiments, alumina powder on micro-polish and polishing pads (Buehler, IL, USA) was used for polishing the electrode. The electrodes were sonicated for 15 min in water, followed by air-drying before use.

2.3.2. Charge/discharge

In this study, systems that were found to exhibit fast kinetics were tested for their charge/discharge characteristics in a small specially fabricated sandwich cell. A Nafion 117 membrane was used as a separator. At the beginning of the charge/discharge, test 20 ml of a solution of 0.1 M $Ce(SO_4)_2$ and 0.03 M DTPA in 1 M H_2SO_4 was pumped into the cathode side. In addition, a 20 ml of solution of 0.1 M $Ce(SO_4)_2$ with 0.03 M DTPA in 2 M H_2SO_4 was pumped into the anode side. Measurements were recorded at a current density of 20 mA cm^{-2}.

3. Results and discussion

3.1. Cyclic voltammetry

A cyclic voltammogram of Ce(IV) in the presence of EDDS at platinum electrode showed anodic and cathodic peaks around 1232 and 490 mV respectively in Fig. 1(a). The anodic peak potential gradually increased from 1228 to 1244 mV with an increase in scan rate. From the standard electrochemistry literature [41,42], Randles–Sevcik equation (1), states that the peak potential is directly proportional to the scan rate, when the scan rate increases the peak potential also increases. The peak current, i_p, is described by the Randles–Sevcik equation as follows:

$$i_p = (2.69 \times 10^5) n^{3/2} A C D^{1/2} \nu^{1/2} \quad (1)$$

where n is the number of moles of electrons transferred in the reaction, A is the area of the electrode, C is the analyte concentration (in mol cm^{-3}), D is the diffusion coefficient, and ν is the scan rate of the applied potential [41,42].

A corresponding cathodic peak potential decrease was observed from 500 to 484 mV with an increase of scan rate from 20 to 300 mV s^{-1} as shown in Fig. 1(b). These changes indicate that the potentials of the anodic and cathodic peaks are dependent upon their scan rates. The symmetric shape of anodic and cathodic peaks reveals good electron transfer but the potential separation (ΔE) shows poor reversibility between the anodic peak and the cathodic peak. The anodic peak current of the Ce(IV)–EDDS complex is larger than the cathodic peak and a variable change from the Ce(IV) is observed. The anodic peak shows a marked increase, whereas there was a slight increase in the cathodic peak current. This means that the addition of EDDS to Ce(IV) was not predominately involved in the chemical reaction.

Rao [11] studied the kinetics of EDTA, DTPA and its analogues by Ce(IV) in sulphuric acid medium using spectrophotometric methods. No electrochemical study has been presented for Ce–DTPA. Rao [11] confirmed that the rate constant depends on the nature of amino groups i.e. tertiary > secondary > primary. This implies that a ligand like NTA, EDTA and EDDS will be less vulnerable to attack by an oxidizing agent like Ce(IV) in sulphuric acid than DTPA. Therefore the Ce(IV)–DTPA complex will be more stable and EDTA.

The Ce(IV)–EDDS results follow the same trend as the Ce(IV)–EDTA results reported earlier [3]. The complexes of Ce(IV)–EDDS and Ce(IV)–EDTA were both electrochemically irreversible, the surface processes are slightly limited and poor linear response encounter by both complexes.

A voltammogram of Ce(IV) in the presence of NTA (Ce(IV)–NTA) is shown in Fig. 2(a). The anodic peak is observed around 1139 mV and the cathodic peak at around 942 mV. The Ce(IV)–NTA complex is electrochemically active, showing a quasi-reversible electrochemical behaviour. The peak current increases with scan rate as

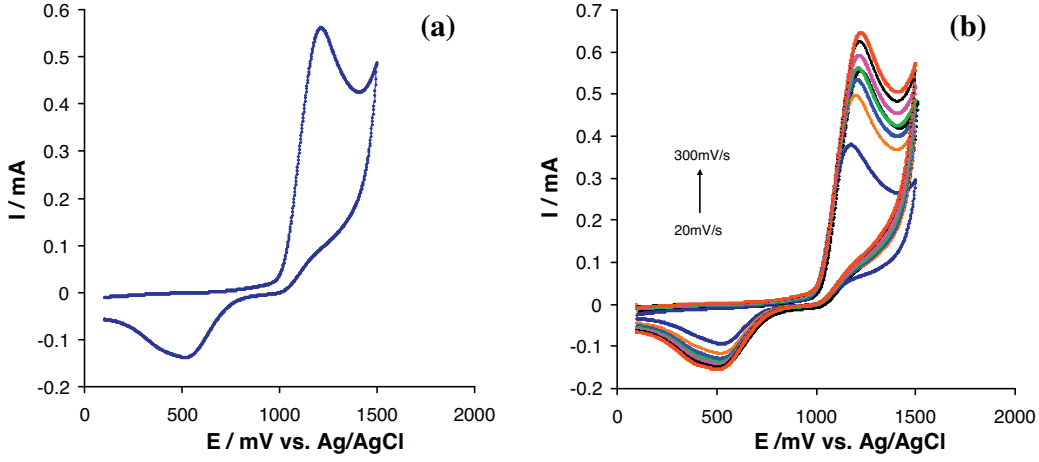

Fig. 1. (a) Cyclic voltammograms of 0.1 M $Ce(SO_4)_2$ solution in 1 M H_2SO_4 with 0.03 M EDDS with a platinum electrode at a scan rate of 100 mV s^{-1} and (b) at scan rates 20, 50, 100, 150, 200, 250 and 300 mV s^{-1}, respectively.

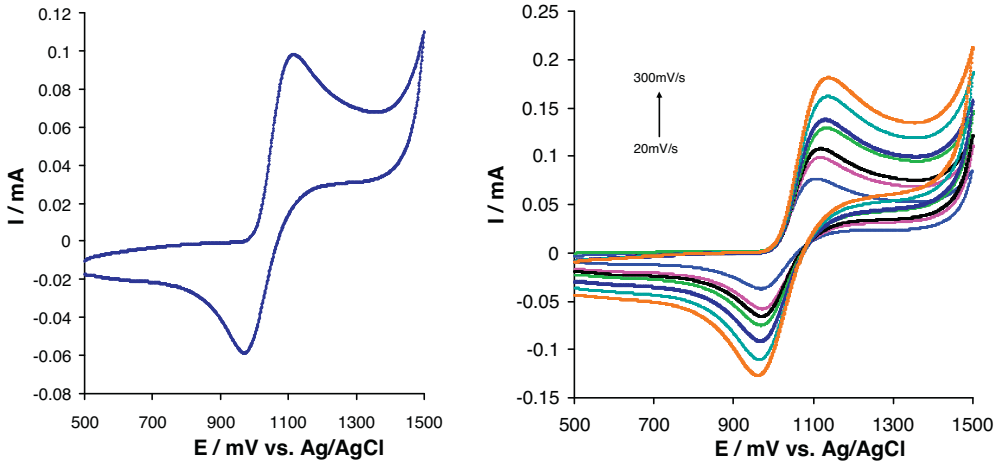

Fig. 2. (a) Cyclic voltammograms of 0.1 M $Ce(SO_4)_2$ solution in 1 M H_2SO_4 with 0.03 M NTA with a platinum electrode at a scan rate of 100 mV s^{-1} and (b) at scan rates 20, 50, 100, 150, 200, 250 and 300 mV s^{-1}, respectively.

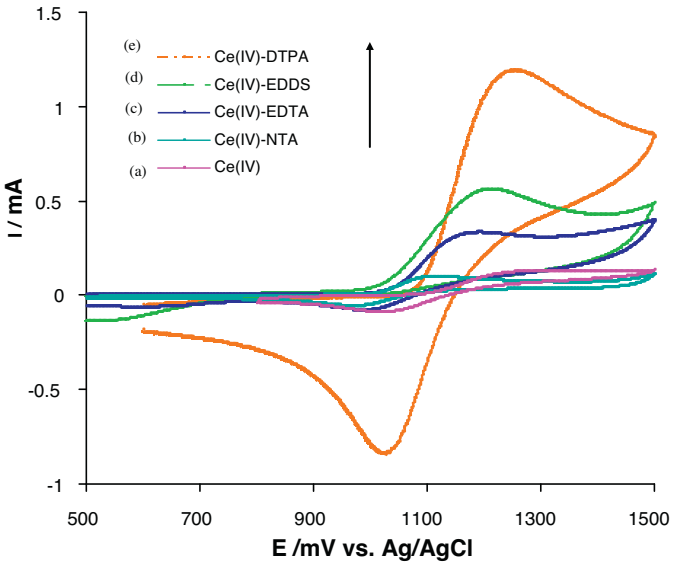

Fig. 3. Cyclic voltammetry at a scan rate of 100 mV s^{-1} (a) CV of 0.1 M $Ce(SO_4)_2$ in 1 M H_2SO_4, (b) CV of Ce(IV)–NTA with 0.03 M NTA, (c) CV of Ce(IV)–EDTA with 0.03 M EDTA, (d) CV of and Ce(IV)–EDDS with 0.03 M EDDS and (e) CV of Ce(IV)–DTPA with 0.03 M DTPA.

seen in Fig. 2(b). Such changes indicate that the potentials of the anodic and cathodic peaks are independent of the scan rate, and the potential separation (ΔE_p) is more than 59 mV. If the potential separation (ΔE_p) is greater than 59 mV the electrochemical reaction is considered to be quasi-reversible. The electrochemical process will be quasi-reversible since the separation between the forward and reverse potential peak (ΔE_p) is greater than 59 m but less than 270, and the potential of the forward peak is independent of the scan rate, according to electrochemistry literature [41,42]. These facts show that the Ce–DTPA is a one electron transfer system according to the well known electrochemical theory [41,42].

A similar cyclic voltammetry shape than that of the Ce(IV)–NTA complex was observed for the Ce(IV)–DTPA complex [3]. Both complexes have good reversible redox reaction, one electron transfer reaction which is mass transfer controlled and diffusion limited in the system.

3.2. Comparison of Ce(IV) with various ligands (EDTA, EDDS, NTA, DTPA)

Ce(IV)–DTPA studies have shown that this complex has promising electrochemical properties; therefore comparison of this complex to others was investigated [3]. A comparison of the cyclic voltammograms for Ce(IV)–DTPA with Ce(IV) as an uncomplexed species, as well as various aminopolycarboxylate ligands (EDTA, EDDS, and NTA), is illustrated in Fig. 3. From forward reaction to the reverse reaction the Ce (IV)–DTPA has a higher potential compared to other complexes. It indicates that the electrochemical reversibility is better than Ce(IV)–EDTA, Ce(IV)–EDDS, Ce(IV)–NTA and Ce(IV) uncomplexed species as shown in Fig. 3. The Ce(IV)–DTPA cyclic voltammograms illustrate a quasi-reversible 1e-transfer reaction electrode process with a potential separation (ΔE_p) of greater than 59 mV, this is the indication of a reversible electrochemical behaviour stated in the literature [41,42].

The Ce(IV)–DTPA complex at various scan rates gave a linear correlation between the peak current (E_p) and the square root of the scan rate, showing that the kinetics of the overall process was diffusion-controlled. Summary of electrochemical parameters and kinetics of the processes is shown in Table 1. The peak ratios of anodic and the cathodic peak for all electrolytes are more than 1, indicating that the anodic reaction is more favourable than the cathodic reaction. The peak potential decrease from Ce(IV)–DTPA > Ce(IV)–NTA > Ce(IV)–EDTA > Ce(IV) > Ce(IV)–EDDS. While the current trend is as follows: Ce(IV)–DTPA > Ce(IV)–NTA > Ce(IV)–EDTA > Ce(IV)–EDDS > Ce(IV). The author [11] confirmed that the rate constant depends on the nature of the amino groups i.e. tertiary > secondary > primary. This implies that a ligand like EDTA and EDDS will be less vulnerable to attack by oxidizing agents like Ce(IV) in sulphuric acid than DTPA and NTA. In addition the Ce(IV)–DTPA complex and Ce(IV)–NTA complex species have higher (k) values than Ce(IV)–EDTA, Ce(IV)–EDDS and Ce(IV) uncomplexed species, meaning that the redox reaction will be faster when DTPA and NTA complexes are used rather than EDTA and EDDS. Therefore, the Ce(IV)–DTPA and Ce(IV)–NTA complex will be more stable and more suitable for redox reaction for flow batteries. However, Ce(IV)–NTA has the lowest current and potential compare to Ce(IV) with other complexes used in this study, hence it will not be suitable as a storage electrolyte for RFB, this is also confirmation from previous results [6].

3.3. Electrochemical impedance spectroscopy

Based on the cyclic voltammetry results, further studies were orientated towards determination of electrolyte resistance using electrochemical impedance spectroscopy. Resistance studies of the five electrolytes Ce(IV), Ce(IV)–EDTA, Ce(IV)–EDDS, Ce(IV)–NTA and Ce(IV)–DTPA were performed and their application in RFB was assessed. In RFB low resistance and fast electron transfer of the electrolyte is favoured. Therefore an electrolyte that has low resistance has superior impedance properties.

3.3.1. Electrochemical impedance spectroscopy of Ce(IV)

The impedance studies of Ce(III)/(IV) redox couple is shown in Fig. 4. The Nyquist plot Fig. 4(a) for the Ce(IV)/Ce(III) couple at different potential from 0.9 V to 1.3 V measured at frequencies of 10^{-1} to 10^5 Hz, displays single semicircles that represent the electron transfer resistance at the electrode surface between the electrolyte/electrode surface from the higher frequency to the lower frequency. This resistance controls the electron transfer kinetics of the redox process at the electrolyte/electrode interface. The highest resistance is normally observed before the redox reaction (1.1 V) in this case at potentials 1.0 and 1.2 V. The capacitance is also lower at 1.1 V where the electron transfer is the fastest. Fig. 4(b)–(c) shows corresponding Bode-magnitude plots, Bode-phase plot and the equivalent electrical circuit model used to determine the resistance. The results fit using the equivalent circuit Fig. 4(d) are presented in Table 2. The higher resistance ($R1$)

Table 1
Electrochemical parameters and kinetics of Ce(IV) in the presence of aminopolycarboxylate ligands with a Pt-electrode.

Electrolyte	E_{pc} (mV)	E_{pa} (mV)	I_{pc} (A)	I_{pa} (A)	$\Delta E = E_a - E_c$ (mV)	I_{pa}/I_{pc}	$D \times 10^6$ ($cm^2\ s^{-1}$)	$k \times 10^4$ (cm^{-1})
Ce(IV)	1002	1252	-8.94×10^{-2}	1.22×10^{-1}	249	1.36	2.4	1.6
Ce–EDTA	982	1192	-3.37×10^{-1}	0.81×10^{-1}	210	2.4	1.3	1.9
Ce–EDDS	490	1223	-1.49×10^{-1}	3.44×10^{-1}	733	2.3	1.5	2.1
Ce–NTA	957	1127	-0.57×10^{-1}	0.97×10^{-1}	170	1.69	1.2	2.6
Ce–DTPA	1080	1264	-7.03×10^{-1}	1.02	184	1.4	1.1	3.1

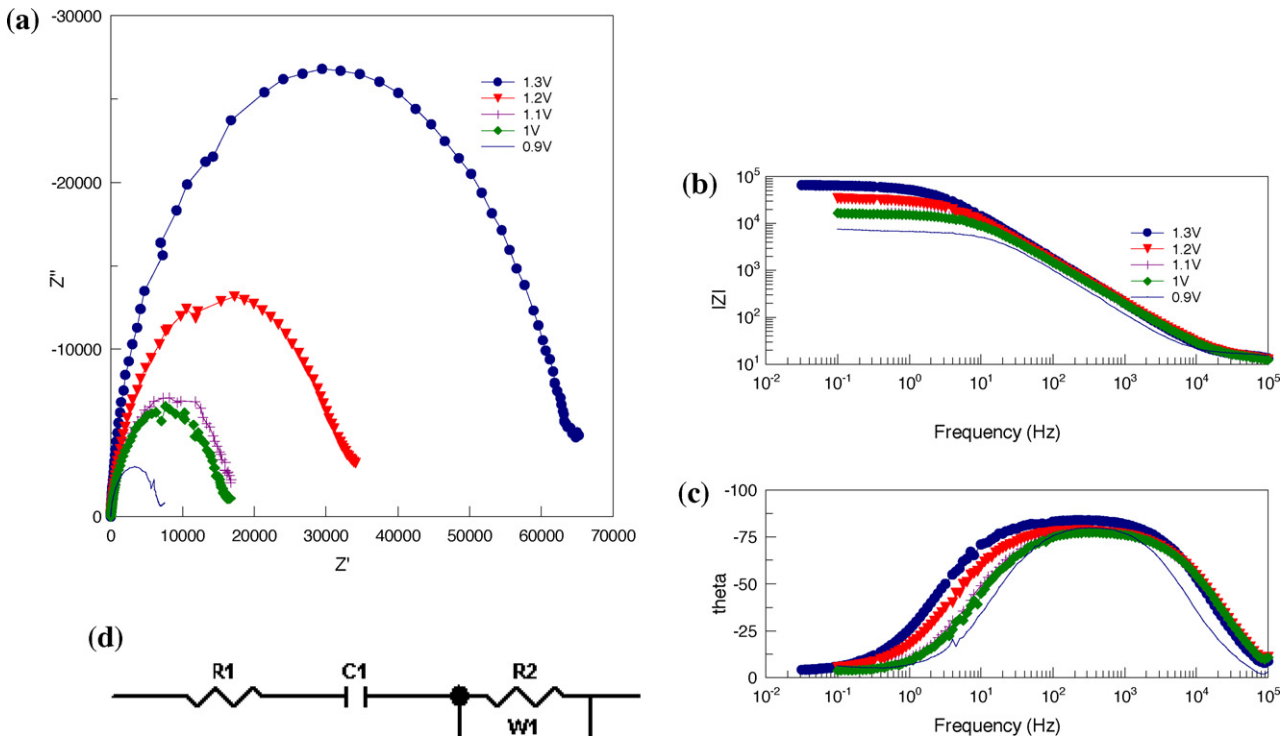

Fig. 4. (a) Nyquist impedance plot of Ce(IV)/Ce(III) couple at different potential from 0.9 V to 1.3 V, (b) Bode-magnitude plot, (c) Bode–phase plot and (d) a equivalent circuit diagram used for fitting the impedance data for the Ce(IV) electrolyte.

between the electrolytes and electrodes was observed at the potential of 1.2 V, *R*2 is also high from 0.9 V to 1.1 V and from 1.2 V to 1.3 V. The % error from 0.18 to 13.79 and the Ce(IV)–EDDS has a higher % error of 9.52 in Warburg diffusion element (*W*1). This is also a confirming by the satisfactory % error of the fitting in Table 2, and all the fitted values were obtained after several circles.

Fig. 5(a) shows the Nyquist plot of a Ce(IV) couple in the presence of EDTA (Ce–EDTA) at different potentials from 0.9 V to 1.3 V. Within the measured frequency range of from 10^{-1} to 10^{5} Hz a single semicircle in the high frequency region is observed. The semicircle presented at high frequency represents the charge transfer process, which is usually described by the charge transfer resistance *R*2. The response at low frequency is related to the diffusion process due to the Ce–EDTA layer that delays the access of the oxidizing species to the surface. At the potential of 1.2 V and 1.3 V the arcs increased with an increase in potential become wider at the high frequency region than at 0.9–1 V at the lower frequency region. At higher frequency the impedance was dominated by the electrolyte resistance, while at low frequency the surface electrode resistance (polarization resistance) was dominating as shown in Fig. 5(b) and (c). Table 3 summarizes the values of the important parameters from equivalent circuit fitting in Fig. 5(d), it was found that the *R*1 value at 1.2 V was the highest than other potentials, *R*2, *C*1 and *W*1 was also higher than other potentials used. The % error of resistance is from 0.15 to 8.48 and the Ce(IV)–EDDS has a higher % error of 9.52 in Warburg diffusion element (*W*1).

3.3.2. Electrochemical impedance of Ce(IV)–DTPA complex

The Nyquist plot of Ce(IV)/Ce(III) couple in the presence of DTPA at different potential from 0.9 V to 1.3 V appears to be a perfect Randles circuit equivalent Fig. 6(a). In the measured frequency range of 10^{-1} to 10^{5} Hz, a single semicircle in the high frequency region and a straight line in the low frequency region for all spectra are observed, except at the potential of 1.3 V where a depressed arc appeared without a straight line. The equivalent circuit is shown in Fig. 6(b) and (c). The corresponding data derived from the measurements of the equivalent circuits is presented in Table 4. The % error of 0.28–8.89 and the Ce(IV)–EDDS has a higher % error of 9.52 in Warburg diffusion element (*W*1). The lowest resistance (*R*1) between the electrolytes and electrodes was observed at a potential of 1.2 V, *R*2 is also low at the potential of 1.2 V, except all other remaining potential, *C*1 and *W*1 values are also high as shown in Table 4. Further study was done to verify that Ce(IV)–DTPA complex shows promise as an electrolyte for redox flow battery. Therefore EIS was used in this work for a more detailed study of the electron transport properties of the electrolyte, given that EIS is the best technique to determine the Ce(IV)–DTPA electrochemical parameters that are reliable.

Table 2
Electrical parameters from circle fitting for the Ce(IV) electrolyte.

E (V)	*R*1 (Ω)	Error %	*R*2 (Ω)	Error %	*C*1 (F cm^{-2})	Error %	*W*1 (Ω)	Error %
0.9	1.332	0.83	2.078	0.74	2.6×10^{-6}	5.18	143.46	2.67
1.0	1.267	0.25	2.348	0.56	2.5×10^{-6}	8.62	101.53	7.84
1.1	1.254	0.85	1.018	2.27	2.3×10^{-6}	11.25	783.5	5.81
1.2	1.474	0.92	3.404	0.25	3.4×10^{-6}	2.51	213.86	3.23
1.3	1.242	0.58	1.036	0.18	2.7×10^{-6}	4.27	143.76	13.79

*R*1: bulk solution resistance, and electrode resistance, *C*1: the capacitance at the contact interface between the electrode and the electrolyte solution (described as a capacitive constant phase element), *R*2: charge transfer resistance in parallel with *C*1, *W*1: Warburg diffusion element *W*1 attributable to the diffusion of ions.

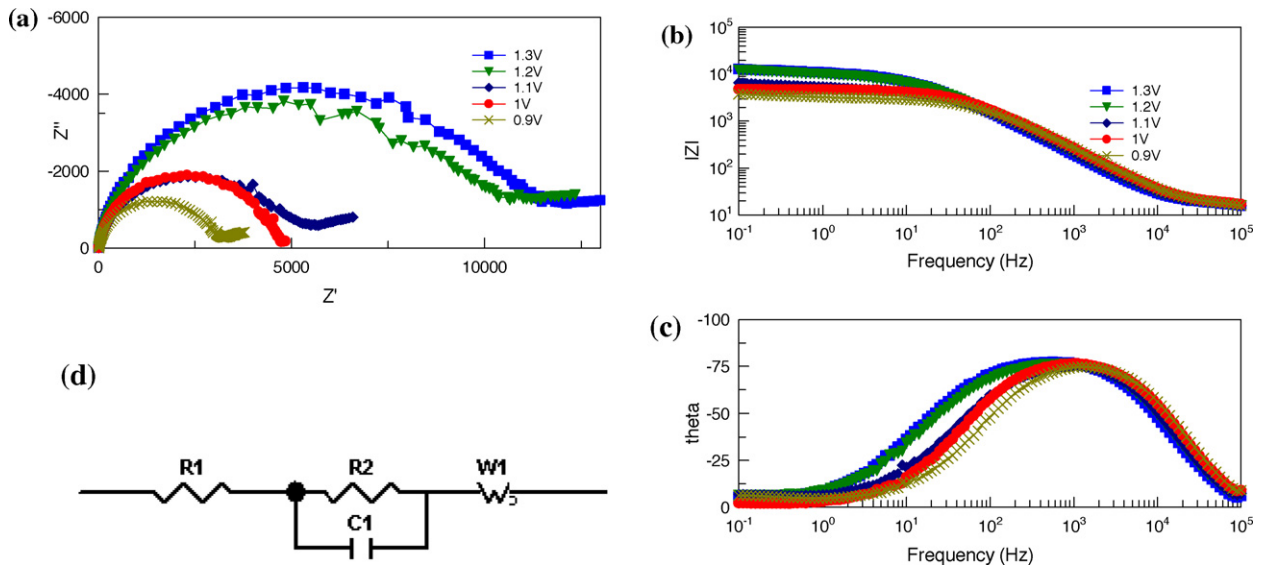

Fig. 5. (a) Nyquist impedance plot of Ce(IV)–EDTA complex at different potential from 0.9 V to 1.3 V, (b) Bode-magnitude plot, (c) Bode-phase plots and (d) a equivalent circuit diagram used for fitting the impedance data for the Ce(IV)–EDTA electrolyte.

Table 3
Electrical parameters from circle fitting for the Ce(IV)–EDTA electrolyte.

E (V)	$R1$ (Ω)	Error %	$R2$ (Ω)	Error %	$C1$ (F cm^{-2})	Error %	$W1$ (Ω)	Error %
0.9	1.442	0.52	2.642	0.82	2.4×10^{-6}	8.88	135.39	5.81
1.0	0.966	0.83	1.9052	1.38	2.3×10^{-6}	4.62	101.35	3.94
1.1	1.125	0.66	2.723	5.62	2.2×10^{-6}	5.25	792.41	9.52
1.2	1.582	0.74	3.562	1.58	2.1×10^{-6}	1.82	225.15	2.89
1.3	1.032	0.15	2.968	8.48	2.5×10^{-6}	3.56	143.57	8.54

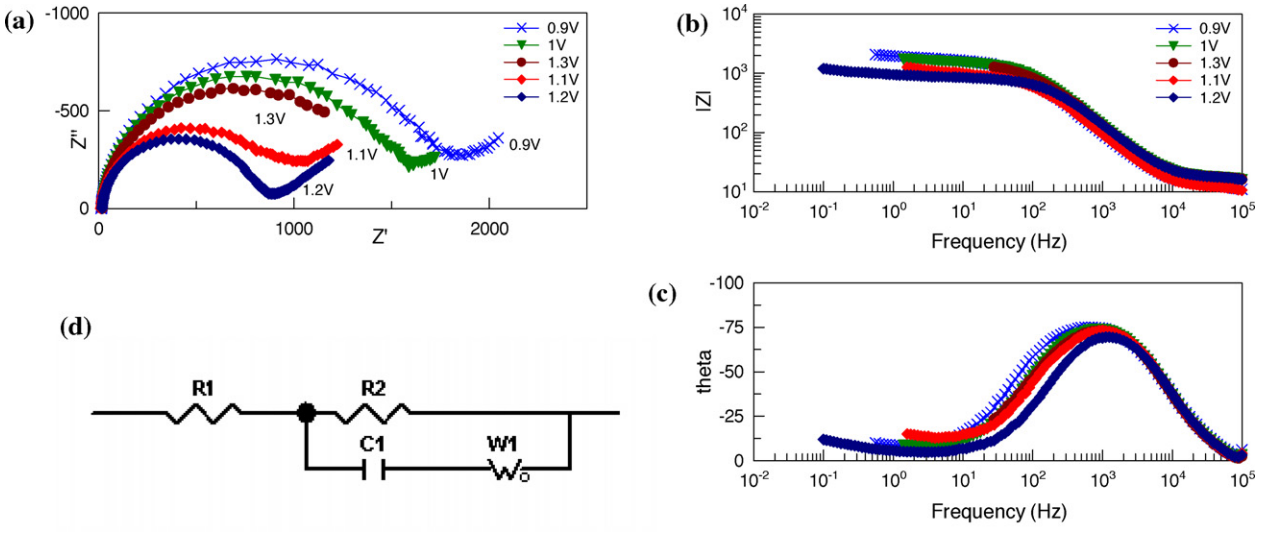

Fig. 6. (a) Nyquist impedance plot of Ce(IV)–DTPA complex at different potential from 0.9 V to 1.3 V, (b) Bode-magnitude plot, (c) Bode-phase plots and (d) a equivalent circuit diagram used for fitting the impedance data for the Ce–DTPA electrolyte.

Table 4
Electrical parameters from circle fitting for the Ce(IV)–DTPA electrolyte.

E (V)	$R1$ (Ω)	Error %	$R2$ (Ω)	Error %	$C1$ (F cm^{-2})	Error %	$W1$ (Ω)	Error %
0.9	1.203	1.12	1.950	0.52	2.6×10^{-6}	2.26	157.28	6.04
1.0	1.198	0.52	1.715	0.38	2.5×10^{-6}	5.42	112.35	5.93
1.1	1.197	1.02	1.802	2.08	2.3×10^{-6}	1.25	829.8	3.02
1.2	1.173	3.04	1.687	2.12	2.3×10^{-6}	8.12	705.5	8.89
1.3	1.205	0.98	1.925	5.06	2.7×10^{-6}	9.82	162.88	6.22

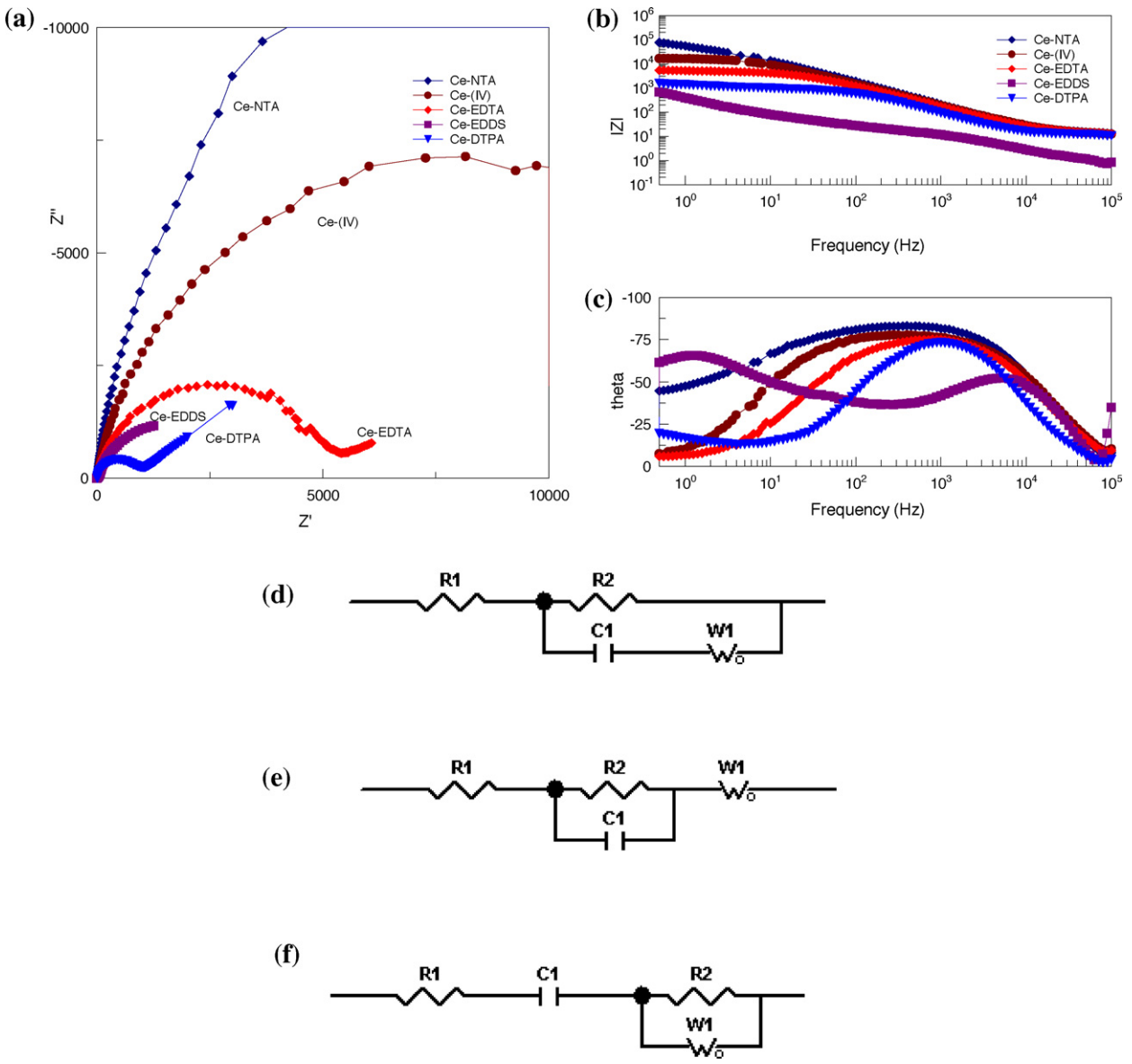

Fig. 7. (a) Nyquist impedance plot for Ce(IV) with (EDTA, EDDS, NTA and DTPA), (b) Bode-magnitude plot, (c) Bode-phase plots and (d–f) equivalent circuit diagrams used for fitting the impedance data (d) Ce–DTPA, (e) Ce(IV), Ce–EDTA, and (f) Ce–EDDS & Ce–NTA.

3.3.3. *Electrochemical impedance studies of the different complexes of Ce(IV) with EDDS, NTA, EDTA and DTPA*

Perfect Randle circuits equivalent circuits characterized by a single semicircle and a straight line appears for all the electrolytes compared, excluding the Ce(IV)–EDDS and Ce(IV)–NTA. A semicircle and a straight line in the electrochemical impedance spectroscopy is shown for Ce(IV)–DTPA and Ce(IV)–EDTA in Fig. 7(a), a single semicircle in the high frequency region and a long straight line with a slope of about 45 °C in the lower frequency region was observed. This is an indication of an electrochemical process that is controlled by an electrochemical reaction and a diffusion step for the Ce(IV)–DTPA complex. Corresponding Bode magnitude plots (logarithm of impedance versus logarithm of frequency) for all complexes are presented in Fig. 7(b) and (c). Data fitting using the circuits depicted in Fig. 7(d)–(f) is summarized in Table 5, with the fitting % error of 0.25–9.52 and the Ce(IV)–EDDS has a higher % error of 9.52 in Warburg diffusion element (*W*1), all the fitted values were obtained after several circles. Ce(IV)–DTPA has the lowest electrolyte resistance (*R*1) and charge transfer resistance (*R*2), *C*1 and *W*1 values are also lower than other in other complexes. Xue et al. [43] pointed out that when the resistance is low the potential will be high, and suggested that when the resistance of the electrolyte is higher, the conductivity of the electrolyte will not be suitable. Based on the above mention finding, the low resistance in Ce(IV)–DTPA will yield higher potential than other complexes used in this study.

3.4. *Charge/discharge performance of cerium redox battery system*

A typical charge/discharge diagram of cerium redox flow batteries that contains Ce(IV) and Ce(IV)–DTPA electrolytes, which are stored in separate electrolyte tanks, and are pumped into the cell. As the cell assembled, it was first charged for 18 h and then discharge as shown in Fig. 8. The current from 10 to 90 mA was appropriate to be utilized, during the discharge process to prevent the cell voltage from dropping rapidly to zero. The current versus time results for the charge/discharge cycles of Ce(IV)–DTPA are shown in Fig. 9. The applied voltage of 0.1–0.9 V was used. From the results it is seen that during charging the current increases with

Table 5
Electrical parameters from circle fitting for various electrolytes.

E (V)	$R1$ (Ω)	Error %	$R2$ (Ω)	Error %	$C1$ (F cm^{-2})	Error %	$W1$ (Ω)	Error %
Ce(IV)	1.474	0.58	3.404	0.35	3.4×10^{-6}	2.25	213.86	6.23
Ce(IV)–NTA	1.351	0.32	3.002	0.38	2.3×10^{-6}	5.52	188.94	8.12
Ce(IV)–EDTA	1.582	0.62	3.562	0.58	2.1×10^{-6}	9.12	225.15	3.05
Ce(IV)–EDDS	1.435	0.94	3.284	0.85	3.2×10^{-6}	7.98	208.52	9.52
Ce(IV)–DTPA	1.173	0.25	1.687	0.52	2.5×10^{-6}	3.58	705.51	4.13

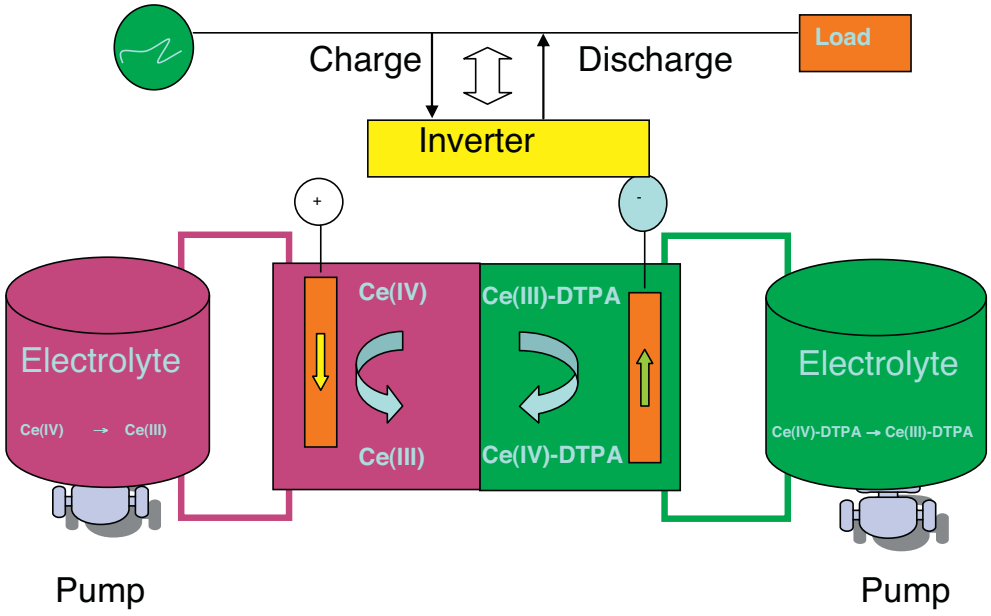

Fig. 8. A typical charge/discharge diagram of Ce(IV) and Ce(IV)–DTPA.

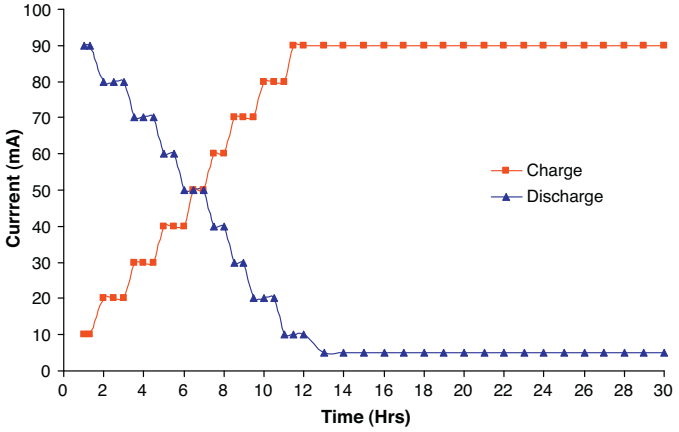

Fig. 9. Charge/discharge curves of the single cell with Ce(IV)–DTPA as redox couples at a current density of 20 mA cm^{-2}.

time from 10 mA to 90 mA and during discharging process the current is gradually decreases from 90 to up to 5 mA. The percentage efficiencies of the Ce(IV), Ce(IV)–EDTA and Ce(IV)–DTPA complex electrolytes used are compared as shown in Table 6, which was previously reported [5]. Therefore from this results it is evident that the percentage energy efficiency for Ce(IV)–DTPA is higher (85%) than other electrolytes used which are Ce(IV), Ce(IV)–EDTA. The coulombic efficiency percentage of Ce(IV) and Ce(IV)–DTPA are the highest than Ce(IV)–EDTA. The Ce(IV)–DTPA system is comparable to the acceptable redox couple currently used in practical RFB systems, without the disadvantages associated with multiple high oxidation state species.

Table 6
Efficiencies of the redox flow battery electrolytes.

Efficiencies (%)	Ce(IV)	Ce(IV)–EDTA	Ce(IV)–DTPA
Coulombic	95	81	92
Voltage	63	45	93
Energy	59	36	85

4. Conclusions

In this study, the electrochemical behaviour of cerium with Ce(IV)–EDTA, Ce(IV)–EDDS, Ce(IV)–NTA and Ce(IV)–DTPA with a platinum electrode were investigated by cyclic voltammetry (CV) and electrochemical impedance spectroscopy (EIS) for use in redox flow batteries (RFB). The reversibility from the CV results was more favourable when Ce(IV) complexed with DTPA ligand compared to the EDTA, EDDS and NTA ligands. Electron transfer was also faster for the Ce(IV)–DTPA complex compared to the other systems calculated from the electron diffusions and standard rate constants. The AC impedance spectra of these redox couples have been analyzed and equivalent circuits were proposed. Equivalent circuit modelling for the Ce(IV)–DTPA complex illustrates that the process taking place is a charge transfer process that is facilitate by a combination of kinetics and diffusion processes. Furthermore the EIS studies have also confirmed the results obtained from CV. The Ce(IV)–DTPA showed the least resistance and faster electron transfer compared to Ce(IV)–EDTA, Ce(IV)–EDDS and Ce(IV)–NTA. Therefore, Ce(IV)–DTPA is a suitable RFB electrolyte compared to Ce(IV), Ce(IV)–EDTA, Ce(IV)–EDDS and Ce(IV)–NTA due to better electrochemical reversibility, lower

resistance, higher potential, kinetics, diffusion control and mass transfer.

Acknowledgments

The authors acknowledge the financial support of the National Research Foundation (NRF), South Africa and the Tertiary Education Support Program (TESP) of the Electricity Supply Commission (ESKOM), University of Stellenbosch, and Sensor Research Group at University of the Western Cape for EIS Instrument.

References

[1] A. Abbaspour, M.A. Mehrgardi, Talanta 67 (2005) 579.
[2] P. Glentworth, B. Wiseall, C.L. Wright, A.J. Mahmood, J. Inorg. Nucl. Chem. 30 (1968) 967.
[3] P. Modiba, A.M. Crouch, J. Appl. Electrochem. 38 (2008) 1293.
[4] P. Modiba, A.M. Crouch, Proceedings of the 43rd Power Source Conference, 2008, p. 71.
[5] P. Modiba, M. Matoetoe, A.M. Crouch, Anal. Lett. 44 (2011) 1967.
[6] P. Modiba, Electrolytes for redox flow battery systems, PhD Thesis University of Stellenbosch, 2010.
[7] P.K. Leung, C. Ponce de León, C.T.J. Low, F.C. Walsh, Electrochim. Acta 56 (2011) 2145.
[8] Y.W.D. Chen, K.S.V. Santhanam, A.J. Bard, J. Electrochem. Soc. 128 (1981) 1460.
[9] Y.W.D. Chen, K.S.V. Santhanam, A.J. Bard, J. Electrochem. Soc. 129 (1982) 61.
[10] T. Yamamura, K. Shirasaki, H. Sato, Y. Nakamura, H. Tomiyasu, I. Satoh, Y. Shiokawa, J. Phys. Chem. 111 (2007) 18812.
[11] A.G.N. Rao, Indian J. Chem. 8 (1970) 328.
[12] J. Li, G. Mailhot, F. Wub, N. Deng, J. Photochem. Photobiol. A: Chem. 212 (2010) 1.
[13] X.X. Ou, X. Quan, S. Chen, F.J. Zhang, Y.Z. Zhao, J. Photochem. Photobiol. A: Chem. 197 (2008) 382.
[14] S. Gangopadhyay, M. Ali, P. Banerjee, Coord. Chem. Rev. 135/136 (1994) 399.
[15] T.J. Egan, S.R. Barthakur, P. Aisen, J. Inorg. Biochem. 48 (1992) 241.
[16] J.L. Pierre, M. Fontacave, Biometals 12 (1999) 195.
[17] F. Neese, E.I. Solomon, J. Am. Chem. Soc. 120 (1998) 12829.
[18] S. Metsarinne, P. Rantanen, R. Aksela, T. Tuhkanen, Chemosphere 55 (2004) 379.
[19] G. Vicente, A. Povse, O. Jose, Trans. Met. Chem. 23 (1998) 657.
[20] M.D. Engelmann, R.T. Bobier, T. Hiatt, I.F. Cheng, BioMetals 16 (2003) 519.
[21] K. Sathiyanarayanan, C. Pavithra, C.W. Lee, J. Ind. Eng. Chem. 12 (2006) 727.
[22] Q. Peng, H. Zhang, J. Chen, Y. Wen, Q. Luo, Z. Liu, Y. Dongjiang, J. Power Sources 175 (2008) 613.
[23] M.H. Chakrabarti, R.A.W. Dryfe, E.P.L. Roberts, Electrochim. Acta 52 (2007) 2189.
[24] M. Skyllas-Kazacos, M. Rychcik, R.G. Robins, A.G. Fane, M. Green, J. Electrochem. Soc. 133 (1986) 1057.
[25] M. Kazacos, M. Skyllas-Kazacos, J. Electrochem. Soc. 136 (1989) 2759.
[26] M. Rychcik, M. Skyllas-Kazaocs, J. Power Sources 19 (1987) 45.
[27] M. Skyllas-Kazacos, M. Rychick, R. Robins, US Patent 4,786,567 (1988).
[28] M. Skyllas-Kazacos, F. Grossmith, J. Electrochem. Soc. 134 (1987) 2950.
[29] M. Skyllas-Kazacos, M. Kazacos, US Patent, 6,562,514 (2003).
[30] M. Rychcik, M. Skyllas-Kazacos, J. Power Sources 22 (1988) 59.
[31] M. Skyllas-Kazacos, Patent Appl. No. PCT/AU88/00472 (1988).
[32] M. Skyllas-Kazacos, C. Menictas, M. Kazacos, J. Electrochem. Soc. 143 (1996) L86.
[33] M. Kazacos, M. Cheng, M. Skyllas-Kazacos, J. Appl. Electrochem. 20 (1990) 463.
[34] T.C. Liu, W.G. Pell, B.E. Conway, Electrochim. Acta 42 (1997) 3541.
[35] B. Fang, S. Iwasa, Y. Wei, T. Arai, M. Kumagai, Electrochim. Acta 47 (2002) 3971.
[36] A. Paulenova, S.E. Creager, J. Power Sources 109 (2002) 431.
[37] D. Pletcher, E. Valder, Electrochim. Acta 33 (1988) 499.
[38] P. Kiekens, L. Steen, H. Donche, E. Temmerman, Electrochim. Acta 26 (1981) 841.
[39] Y. Wei, B. Fang, J. Appl. Electrochem. 35 (2005) 561.
[40] D. Pletcher, J.C.P. White, Electrochim. Acta 37 (1992) 575.
[41] J. Bard, L.R. Faulkner, Electrochemical Methods Fundamentals and Applications, 2nd edition, John Wiley & Sons, New York, 2001.
[42] P. Zanello, Inorganic Electrochemistry Theory, Practice and Application, The Royal Society of Chemistry, Cambridge, 2003.
[43] F.-Q. Xue, Y.-L. Wang, W.-H. Wang, X.-D. Wang, Electrochim. Acta 53 (2008) 6636.